World Scientific Research Journal Volume 11 Issue 8, 2025
ISSN: 2472-3703 DOI: 10.6911/WSRJ.202508_11(8).0001

Design and Optimization of Bionic Pressing Roller

Lu Gao[1, 2, a], Yuchen He[2], Yiding Shi[2] and Manxi Sun[2]

[1]School of Mechanical Engineering, Xihua University, Chengdu 610039, China

[2]Institute of Modern Agricultural Equipment, Xihua University, Chengdu 610039, China

[a]2662682283@qq.com

Abstract

Aiming at the high resistance and "soil accumulation" phenomenon existing in the operation of the traditional potato harvester's pressing roller, this study, based on the non-smooth surface characteristics of the grub and combined with bionics principles to extract the structural features of its back convex hull, designed a bionic pressing roller. The surface morphology of the grubs was obtained by a 3D contour scanner. A roller model with a diameter of 110mm and a width of 580mm was constructed, and the finite element model of the pressing roller - soil was established by using ABAQUS software (the Drucker-Prager constitutive model was adopted for the soil). The simulation results show that the bionic pressure roller effectively eliminates the soil accumulation phenomenon and significantly reduces the working resistance compared with the traditional cylindrical roller. Further through single-factor tests and Box-Behnken response surface optimization, the optimal parameter combination was determined to be a convex hull height of 15mm, an operating speed of 0.72m/s, and a suppression load of 320N. At this time, the traction resistance was 228.64N, verifying the superiority of the bionic structure in drag reduction and surface leveling.

Keywords

Bionic pressing roller; Finite element simulation; Grubs; Response surface experiment.

1. INTRODUCTION

With the rapid development of agriculture, the mechanized production level of potatoes in China has gradually improved. Up to now, both the planting scale and annual output rank first in the world [1]. In the hilly areas of southwest China, segmented harvesting is mostly adopted, generally consisting of three parts: weeding, digging and manual picking. During the excavation process, potatoes are scattered onto the freshly excavated ground after being shaken (tuber and soil separation). Installing a pressing roller under the shaking screen to level the ground can effectively prevent potatoes from being overly scattered and reduce the chance of them being crushed by the tractor. During the operation of traditional cylindrical rollers, wavy protrusions will appear at the front, which is called the "soil accumulation" phenomenon. During the process of pushing the soil, not only does it prevent the rollers from achieving the desired compaction effect, but it also causes the rollers to consume more work to push the raised soil [2]. Jack Ellwood Steele proposed the definition of bionics in 1960 [3] : Bionics is the construction of various cave animals [4] by imitating the principles of biological systems, such as earthworms, dung beetles, pangolins, and grubs, which can move freely in the soil without their bodies being clay. This provides a new idea for the de-adhesion and desorption of the soil-contacting parts of agricultural machinery [5] Based on the problems such as severe soil adhesion and high operation resistance during the operation of the potato harvester's pressing roller, and considering that grubs [6] live in the soil and their surfaces are basically not clay, a bionic

ISSN: 2472-3703 DOI: 10.6911/WSRJ.202508_11(8).0001

pressing roller was designed by extracting the surface shape features of grubs. The response surface simulation test was conducted using the finite element analysis software ABAQUS to optimize the convex hull structure of the pressing roller, and the optimal structure and working parameters were obtained.

2. DESIGN OF BIONIC PRESSING ROLLER

This paper uses reverse engineering technology as a tool to complete the reconstruction task of the surface structure model of the sample object, and constructs the contour structure model of the protrusion on the back of the wireworm [7]. The specific tool used is the 3D contour measuring instrument of Sixian Optoelectronic Technology Co., LTD. The measurement mode is selected as "displacement mode", the measurement mileage is selected as 4mm, and the sampling frequency is selected as 500Hz. The rest keep the default options. The basic situation of the 3D profilometer and the grub sample are shown in Figure 1.

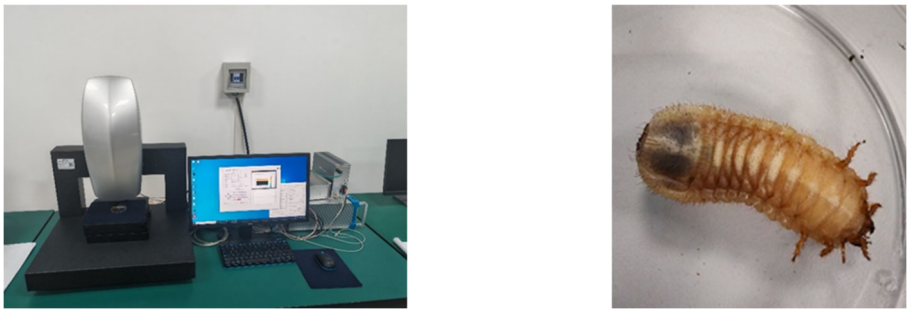

(a) 3D contour scanner (b) Grub sample

Figure 1. Schematic diagram of 3D scanner instrument and wireworm sample

The convex hull structure on the back of the grub was scanned by a 3D profile scanner to obtain its back contour features. The contours with more obvious protrusions (see the horizontal axis of Figure 2, which is 1mm-1.5mm) were selected and smoothed using MATLAB software.

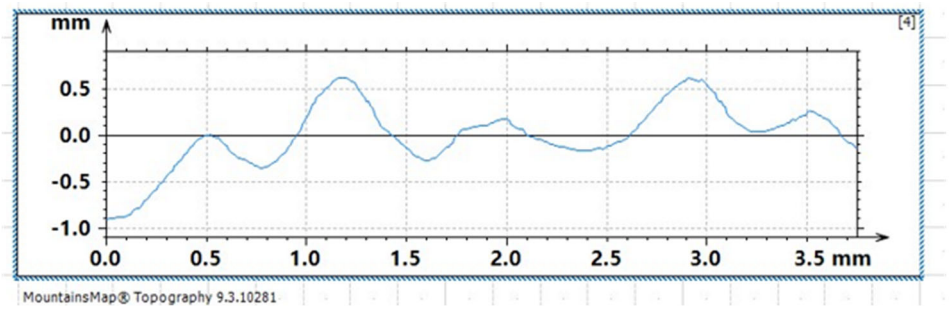

Figure 2. Cross-sectional curve of the surface scanning result of grubs

A bionic pressure roller was designed, as shown in Figure 3 (a). Based on the structural dimensions of the machine and the cylindrical steel pipe, the diameter of the pressing roller was selected as 110mm, the width as 580mm, and the inner diameter as 94mm. The designed bionic pressing roller is shown in Figure 3 (b).

ISSN: 2472-3703 DOI: 10.6911/WSRJ.202508_11(8).0001

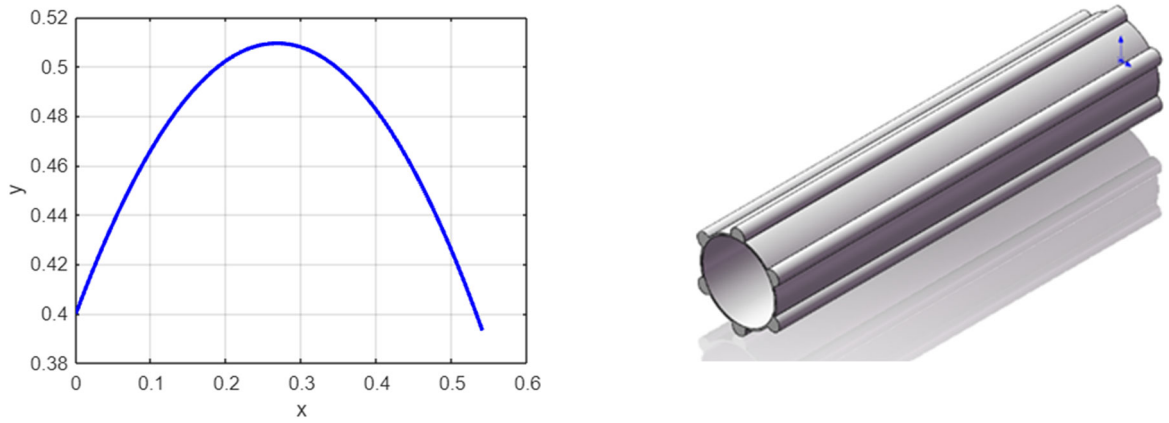

(a) Convex hull curve (b) Bionic pressing roller model diagram

Figure 3. Convex hull curve and bionic pressure roller model diagram

3. ESTABLISHMENT OF THE FINITE ELEMENT MODEL

3.1. Pressing roller

Based on the dimensions of the traditional pressing roller used in the potato harvester and the designed bionic pressing roller, a three-dimensional model was established in the ABAQUS software. The outer diameter of the traditional pressure roller and the bionic pressure roller is 110mm, the width is 580mm, and the thickness is 8mm. The surface of the bionic pressure roller is designed by extracting the convex bulge features on the surface of the grubs. After the model is built, the grid is divided, a hexahedral mesh was selected, with the mesh size set at 5mm, and the free mesh division technology was adopted for division, as shown in Figure 4.

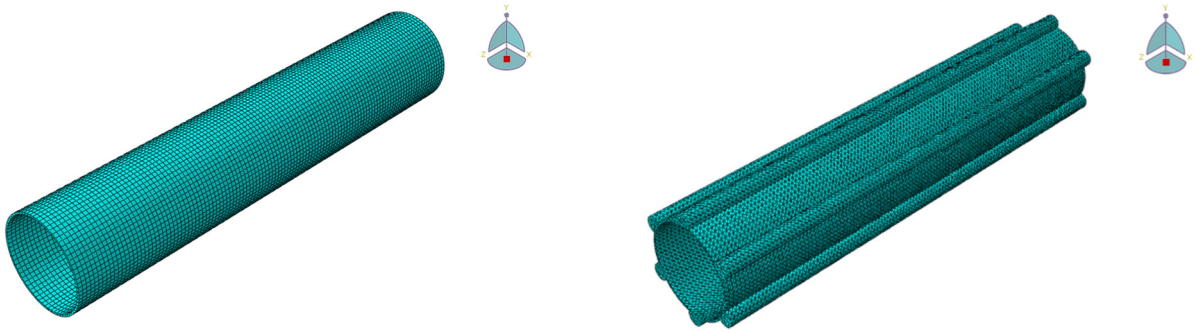

(a) Traditional pressing roller (b) Bionic pressing roller

Figure 4. Schematic diagram of grid division for the pressing roller

3.2. Soil

3.2.1 Soil parameters

During the simulation process, when the soil and the compaction roller come into contact with each other, the soil will deform, and this deformation will affect the operation of the compaction roller. That is, the soil model in the simulation process directly affects the simulation effect. Therefore, soil is regarded as an elastoplastic body, and the Drucker-Prager model [8] is selected for its constitutive model, and its parameters are shown in Table 1.

ISSN: 2472-3703 DOI: 10.6911/WSRJ.202508_11(8).0001

Table 1. Soil parameters

Parameters	Value	
Mass density (t/mm3)	1.3e-9	
Young modulus (Mpa)	1.75	
Poisson ratio	0.41	
Friction Angle (°)	28.2	
Flow stress ratio	1	
Expansion Angle (°)	0	
Drucker-Prager hardening sub-option	Yield stress (Pa)	Absolute plastic strain
	8670	0
	169980	143.78
	249970	211.4
	309980	262.12
	379930	321.3

3.2.2 Three-dimensional soil model and grid division

The soil model is 1500mm in length, 1000mm in width and 200mm in height. Before grid division of the soil, the soil model is divided into two parts. The upper half (50mm) of the soil area close to the roller is subdivided into grids using structured grid division technology, with the size of the grid cells being 10mm. The soil area far from the roller soil action zone (150mm in the lower half) adopts the sweeping grid division technology, with the grid cell size ranging from 10 to 50mm. Moreover, the nodes in the upper half are defined as a set to provide a basis for the subsequent contact setting. The grid division and soil nodes are shown in Figure 5.

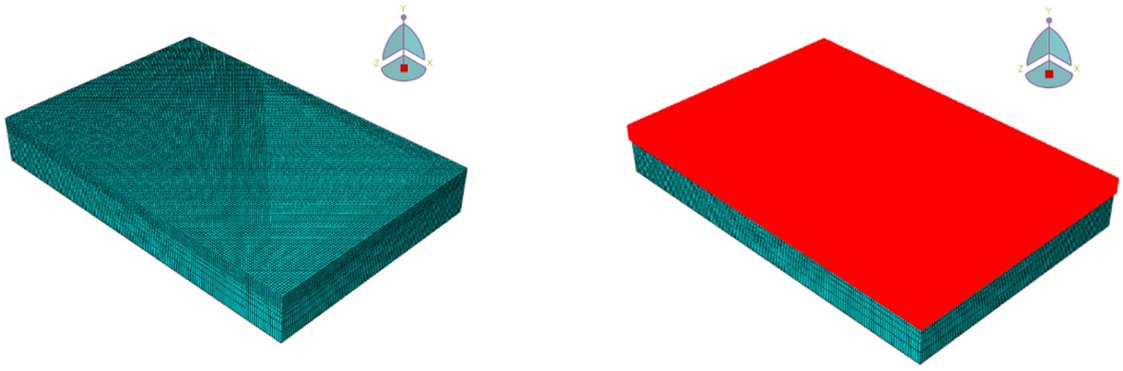

(a) Grid division (b) Soil nodes

Figure 5. Schematic diagram of grid division and nodes

3.3. Boundary conditions and loading methods

3.3.1 Pressing roller

Create two subsequent analysis steps to apply load and speed to the reference point of the pressing roller respectively. In the first subsequent analysis step, a load of 300N was applied to establish a contact relationship between the compaction roller and the soil, with the time set at 0.2 seconds. In the second subsequent analysis step, a forward speed of 0.9m/s is applied to the pressure roller, with the time set at 1 second.

3.3.2 Soil

In the initial analysis step that comes with the system and the creation of two subsequent analysis steps, all the degrees of freedom at the bottom of the soil are fully restricted, and no constraints are added to the remaining surfaces.

ISSN: 2472-3703 DOI: 10.6911/WSRJ.202508_11(8).0001

3.3.3 Define contact

The contact algorithm adopts the face-to-face contact algorithm, selecting the outer surface of the compaction roller as the main surface and the upper node area of the soil region in contact with the compaction roller as the secondary surface. The normal interaction between the contact surfaces is defined as "hard contact", the tangential interaction as the penalty function method and the Coulometric friction model, and the coefficient of friction is set to 0.42. Other options in the contact properties are selected by default.

3.4. Comparison of results

Under the same conditions, the compaction effects of traditional cylindrical compaction rollers and bionic convex package compaction rollers after operation are quite different. Bionic compaction rollers basically do not produce the "soil accumulation" phenomenon, while traditional compaction rollers produce a more obvious "soil accumulation" phenomenon. The effects of the two assignments are shown in Figure 6.

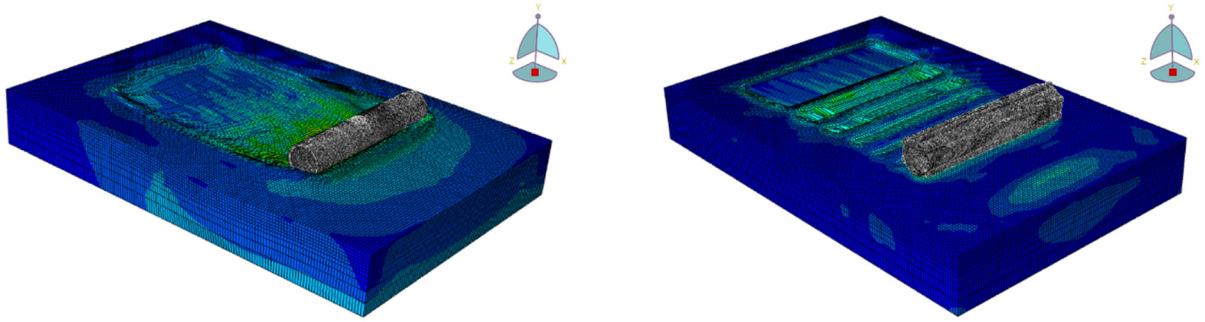

(a) Operation effect drawing of the traditional pressing roller

(b) Operation effect drawing of the bionic pressing roller

Figure 6. Comparison chart of the working effects of traditional and bionic pressing rollers

4. DETERMINE THE STRUCTURAL PARAMETERS OF THE BIONIC PRESSING ROLLER

To explore the influence of the structural parameters of the bionic pressure roller on its resistance during operation, a single-factor simulation test was conducted. With the height, width, number of bumps, operation speed and pressure load of the bumps as the test variables and the rolling resistance as the test index, the single-factor simulation test was carried out. The test results are as follows.

4.1. Single-factor simulation test

4.1.1 The influence of the convex hull height

The test variable is the height of the convex hull, and the test levels are 12, 13, 14, 15, and 16mm respectively. Taking the traction resistance as the evaluation index, a single-factor five-level simulation test is conducted under the conditions of an operating speed of 0.9m/s, a suppression load of 300N, a number of 6 convex hull, and the remaining structural parameters are consistent with the simulation parameters. The results are shown in Table 2.

ISSN: 2472-3703 DOI: 10.6911/WSRJ.202508_11(8).0001

Table 2. The influence of the convex hull height on traction resistance

number	Convex hull height (mm)	Traction resistance (N)
1	12	410.26
2	13	409.33
3	14	377.20
4	15	394.71
5	16	395.22

Within a certain range, as the height of the convex hull increases, the traction resistance decreases. When the traction resistance drops to a certain value, the working resistance increases accordingly. This is because during the operation of the roller, when the height of the bump increases to an appropriate value, the contact area between the roller and the soil decreases, the "soil accumulation" phenomenon significantly reduces, and the required pushing force also decreases accordingly, thereby reducing the working resistance. However, when the height of the bump increases too much, the contact area between the roller and the soil decreases sharply, causing the ground pressure of the roller to be too high and thus increasing the working resistance.

4.1.2 The influence of the width of the bulge

The test variable was the width of the convex hull, and the test levels were 16, 17, 18, 19 and 20mm respectively. The traction resistance was used as the evaluation index. Under the conditions of an operating speed of 0.9m/s, a compressive load of 300N, 6 convex hull numbers, a convex hull height of 14mm, and the remaining structural parameters being consistent with the simulation parameters, a single-factor five-level simulation test was conducted. The results are shown in Table 3.

Table 3. The influence of convex hull width on traction resistance

number	convex hull width (mm)	Traction resistance (N)
1	16	408.42
2	17	393.08
3	18	377.20
4	19	385.63
5	20	400.17

As is evident from the above table, during the progression of continuously increasing the width of the convex hull, the traction resistance initially decreases and subsequently increases. Nevertheless, the variation in traction resistance is not particularly notable with the change in width. In light of the previous research and design of the compaction roller by scholars, the width of the convex hull is chosen to be 18 mm.

4.1.3 The influence of the number of protrusions

The test variable is the convex hull width, and the test levels are 4, 5, 6, 7, and 8 respectively. Take traction resistance as the evaluation index. Under the conditions of a running speed of 0.9m/s, a compressive load of 300N, a convex hull height of 14mm, a convex hull bottom width of 18mm, and the remaining structural parameters being consistent with the simulation parameters, a single-factor five-level simulation test was conducted. The results are shown in Table 4.

ISSN: 2472-3703 DOI: 10.6911/WSRJ.202508_11(8).0001

Table 4. The influence of the number of protrusions on traction resistance

number	Number of protrusions (pieces)	Traction resistance (N)
1	4	471.40
2	5	430.90
3	6	377.20
4	7	485.10
5	8	554.05

It can be observed from the above table that as the number of convex hulls continuously increases, the traction resistance first decreases and then increases. When analyzed in conjunction with the finite -element process variables, it is evident that when the number of convex hulls is less than six, the compaction roller is in a "suspended" state during operation. That is to say, there are portions of the soil that remain uncompacted during the operation, resulting in an unsatisfactory compaction effect. Hence, the number of convex hulls is set to six.

4.1.4 The influence of work speed

The test variable is the operating speed, and the test levels are 0.3, 0.5, 0.7, 0.9, and 1.1m/s. The traction resistance is used as the evaluation index. Under the conditions of a compressive load of 300N, a width of the bottom surface of the convex hull of 18mm, a height of 14mm, a number of 6 convex hull, and the remaining structural parameters being consistent with the simulation parameters, a single-factor five-level simulation test is conducted. The results are shown in Table 5.

Table 5. The influence of operation speed on traction resistance

number	Operation speed (m/s)	Traction resistance (N)
1	0.3	183.52
2	0.5	258.82
3	0.7	326.03
4	0.9	377.20
5	1.1	446.97

As can be seen from the above table, as the operation speed keeps increasing, the traction resistance also keeps growing. This is because a slower speed results in a shorter operation distance within the same period of time. Combining the operation speeds of the potato harvester and the tractor, the operation speed of 0.5-0.9m/s is initially selected as the level of operation speed for the response surface simulation test.

4.1.5 The influence of the suppression load

The test variable is the suppression load, and the test levels are 200, 300, 400, 500, and 600 N. The traction resistance is used as the evaluation index. Under the conditions of an operating speed of 0.9m/s, a width of the bottom surface of the convex hull of 18mm, a height of 14mm, a number of 6 convex hull, and the remaining structural parameters being consistent with the simulation parameters, a single-factor five-level simulation test is conducted. The results are shown in Table 6.

ISSN: 2472-3703 DOI: 10.6911/WSRJ.202508_11(8).0001

Table 6. The influence of suppression load on traction resistance

number	Suppression load (N)	Traction resistance (N)
1	200	330.85
2	300	377.20
3	400	930.54
4	500	1785.12
5	600	2502.58

It can be seen from the above table that as the compressive load keeps increasing, the traction resistance keeps rising. Combined with the finite element process variables, it can be observed that when the compressive load is 200N, the traction resistance output is 0 at some time points, which can be inferred that the compaction is insufficient. When the suppression load is 600, the traction resistance is too large, resulting in an increase in the extra work done. Therefore, the suppression load of 300-500N is initially selected as the response surface to simulate and test the level of the suppression load.

4.2. Box-Behnken central composite design experiment

4.2.1 Experimental factors and metrics

The Box - Behnken central composite experimental design was carried out using the Design - Expert software. To evaluate the drag - reducing characteristics of the bionic press roller, the average traction resistance of the press roller during normal operation (from 0.2s to 1s) in the simulation process was adopted as the experimental indicator.According to the results of the above single - factor simulations, the number of convex structures was set at 6, and the bottom width of each convex structure was 18mm. Since these two factors have little impact on the traction resistance, further experimental investigations on them were not conducted. After consulting relevant literature and considering the actual situation, three factors, namely the height of the convex structures on the press roller, the operating speed, and the load, were selected as experimental factors to conduct a three - factor, three - level Box - Behnken central composite experiment.

4.2.2 Experimental protocol

The height of the convex structures, operating speed, load, and traction resistance are denoted as A, B, C, and f, respectively. The height of the convex structures spans a level range of 14 - 16 mm, the operating speed ranges from 0.5 to 0.9 m/s, and the load ranges from 300 to 500 N. The coding table for the simulation test factors is presented in Table 7, and the results of the simulation tests are shown in Table 8.

Table 7. Coding Table of Experimental Factors

Level	Factors		
	Convex hull height (mm)	Operating speed (m/s)	Suppressive load (N)
-1	14	0.5	300
0	15	0.7	400
1	16	0.9	500

ISSN: 2472-3703 DOI: 10.6911/WSRJ.202508_11(8).0001

Table 8. Simulation test plan and results

Test Serial Number	Convex hull height (mm)	Operating speed (m/s)	Suppressive load (N)	Traction resistance (N)
1	16	0.9	400	461.6
2	15	0.7	400	392.39
3	14	0.7	500	1306.13
4	15	0.7	400	329.39
5	16	0.7	500	793.35
6	16	0.7	300	328.49
7	14	0.7	300	326.03
8	15	0.9	300	304.5
9	15	0.5	500	564.02
10	15	0.5	300	260.94
11	14	0.9	400	930.54
12	15	0.9	500	1230.46
13	15	0.7	400	329.39
14	14	0.5	400	709.8
15	16	0.5	400	313.21

4.2.3 Analysis of test results

A variance analysis was conducted on the traction resistance, and the results are shown in Table 8. According to the variance analysis results, the significance P value of the traction resistance f is less than 0.01, which is extremely significant, indicating that the model has statistical significance. The model's determination coefficient R^2 is 0.9725, and the adjusted determination coefficient R^2adj is 0.9231, suggesting that the model has high reliability.

Table 9. Results of the Analysis of Variance (ANOVA) for Traction Resistance

	df	Sum of Squares	Mean Squares	F-value	P-value	
Model	9	1.596e6	1.773e5	19.68	0.0022	**
A	1	2.366e5	2.366e5	26.27	0.0037	**
B	1	1.456e5	1.456e5	16.16	0.0101	*
C	1	8.938e5	8.938e5	99.22	0.0002	**
AB	1	1308.63	1308.63	0.1453	0.7188	not significant
AC	1	66368.06	66368.06	7.37	0.0421	*
BC	1	96994.87	96994.87	10.77	0.0219	*
A2	1	88527.03	88527.03	9.83	0.0258	*
B2	1	11712.65	11712.65	1.30	0.3058	*
C2	1	73442.78	73442.78	8.15	0.0356	*
Pure Error	2	8919.22	4459.61			
Lack of Fit	3	12041.16	36123.49	2.70	0.2818	not significant
Cor Total	14	1.641e06				

Note: $P < 0.01$ (extremely significant, **), $P < 0.05$ (significant, *), $P > 0.05$ (not significant)

From the variance analysis table, the larger the F value, the greater the influence of the factor on the traction resistance. The significance of the influence of each factor and factor interaction on the traction resistance of the compaction roller, from greatest to least, is: operating load, the convex hull height, operating speed. By eliminating the insignificant items in Table 7, the multiple regression equation for the traction resistance f is obtained as:

ISSN: 2472-3703 DOI: 10.6911/WSRJ.202508_11(8).0001

$$f = 392.62 - 171.98A + 134.89B + 334.25C - 128.81AC + 155.72BC + 154.84A^2 + 56.32B^2 + 141.03C^2 \quad (1)$$

The data were processed using Design-Expert software to derive the response surface depicting the influence of relatively significant interaction factors on the experimental indicators. Regarding the working resistance f, when the forward speed is 0.7m/s, the interaction effect surface between the convex hull height and the load is presented in Figure 10. When the convex hull height is held constant, as the load increases, the working resistance also rises. This is attributable to the fact that during the operation of the bionic compaction roller, the movement of soil particles is constrained by the frictional forces among them. Soil particles do not exhibit extensive movement. As the load increases, the frictional forces between soil particles increase accordingly. Consequently, the compaction roller requires a greater force to carry out the compaction operation, thereby increasing the working resistance of the compaction roller. When operating under a specific load, the traction resistance initially decreases and then increases, which aligns with the aforementioned single-factor experiment. The reasons for this phenomenon will not be elaborated further herein. From the overall trend of the response surface, the variation trend of the traction resistance on both sides of the response surface is relatively steep. This indicates that both factors have a notable influence on the traction resistance.

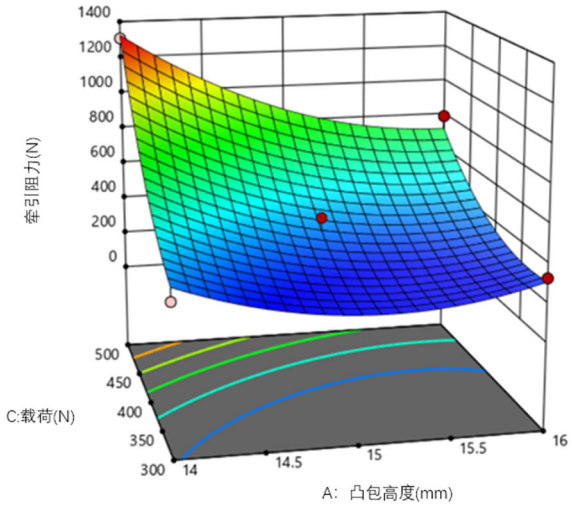

Figure 5. The Two-Factor Response Surface for Traction Resistance

The smaller the working resistance of the bio-inspired convex-hull structured compaction wheel, the lower the energy consumption required during operation. To determine the optimal kinematic and structural parameters of the bionic compaction wheel, the optimization module within the Design - Expert software was employed to optimize and solve the regression models of the working resistance and settlement. Among the highly reliable results, considering the manufacturing process, a set of optimal parameter combinations was selected. The findings indicate that when the forward speed of the machine is 0.72 m/s, the load is 320 N, and the convex-hull height is 15 mm, the traction resistance is 234.17 N. Validation through finite element simulation yielded a traction resistance of 228.64 N, showing a minor discrepancy from the predicted value.

ISSN: 2472-3703 DOI: 10.6911/WSRJ.202508_11(8).0001

5. SUMMARY

This paper addresses the issue that traditional soil compaction rollers tend to adhere soil during operation, causing soil accumulation and high operational resistance, which fails to achieve the desired compaction effect. By integrating the principles of bionics and using a three-dimensional profilometer to extract the protruding structures on the surface of the grub, a bionic soil compaction roller was designed. Dynamic simulation of the compaction roller was conducted using the ABAQUS finite element simulation software. The simulation results show that the bionic compaction roller hardly causes soil accumulation, while the traditional compaction roller does. Additionally, single-factor simulation experiments were carried out to explore the height, width, and quantity of the protrusions on the bionic compaction roller. Based on the single-factor simulation experiments, a BBD central composite design experiment was conducted, and the optimal structure and working parameters of the bionic compaction roller were obtained: protrusion height of 15mm, operating speed of 0.72m/s, and load of 320N, with a traction resistance of 234.17N at this time. The finite element simulation verified that the traction resistance was 228.64N, indicating that the obtained structure and working parameter combination is reasonable.

ACKNOWLEDGMENT

We acknowledge the support of Integrated Pilot Project of Sichuan Provincial Department for Research, Manufacturing, Promotion, and Application of Agricultural (CNH[2024]582-2 and CNH [2024]582-3).

REFERENCES

[1] Yuan Zhong, Sun Ying, Bai Yun Design and Experiment of Vibrating Potato Harvester Based on EDEM [J]. Agricultural Mechanization Research, 24,46(12):167-173.

[2] Zhang Qingzhu. Soil Compaction Roller with Biomimetic Geometric Structure Surface [D]. Jilin University, 2014.

[3] Liu Hongjun. Research on Key Technologies of Seeding Machine Pressing Device in Northeast Hilly Region [D]. Northeast Agricultural University, 2019.

[4] Steele M J E. How do we get there[C]. Bionics Symposium, Dayton Ohio In Gray C.H. Figueroa-Sarriera H, Mentor, S.(1995)The Cyborg Handbook New York: Routledge. 1960: 55-59.

[5] Liu Lu, Wang Lianji, Hu Hong, et al. Research Status and Prospect of Bionic Viscosity Reduction Technology for Soil Contact Parts of Agricultural Machinery [J]. Agricultural Equipment and Vehicle Engineering,2022,60(07):27-31.

[6] Qiu Shaojie Research on Adhesion and Friction Characteristics on the Surface of Grubs [D]. Nanjing University of Aeronautics and Astronautics,2019.

[7] Chen Jiaqi. Design and Experiment of Bionic Convex Hull Structure Pressure Wheel [D]. Northeast Agricultural University,2019.

[8] Bing Shulong. Design and Experimental Research on the Soil Covering and Compaction Device of the Oil Sand Bean Planter [D]. Jilin Agricultural University,2023.